

Oxidative degradation of *N*^ε-fructosylamine-substituted peptides in heated aqueous systems

Uta Greifenhagen · Andrej Frolov · Ralf Hoffmann

Received: 11 December 2014 / Accepted: 11 February 2015 / Published online: 25 February 2015
© Springer-Verlag Wien 2015

Abstract Glycation, or non-enzymatic glycosylation, is a common protein modification formed by reactions between reducing sugars (i.e. aldoses and ketoses) with protein amino groups. Resulting Amadori and Heyns compounds, respectively, can be oxidatively degraded yielding a structurally heterogeneous group of advanced glycation end-products. We have studied this process in aqueous conditions at 95 °C in terms of appearing products and their formation kinetics in the presence or absence of reactive oxygen species (ROS)-generating systems (iron(II) sulfate). RP-HPLC–ESI–MS revealed 20 products, 12 of which were confirmed after synthesis by identical retention times and fragmentation patterns. These products accumulated during the incubation period of 4 h (*N*^ε-carboxymethyl-, *N*^ε-formyl- and *N*^ε-methyl lysine) or appeared intermediately (2-aminoadipic semialdehyde, *N*^ε-ethanalyl lysine). Acidic and basic amino acid residues near the glycation site and elevated ROS levels in the reaction mixture had significant effects on both product formation and degradation kinetics.

Keywords Advanced glycation end-products (AGEs) · Amadori product degradation, glycation · Glucose · Non-enzymatic post-translational modification · Reactive oxygen species (ROS)

Introduction

Protein glycation is an ubiquitous post-translational modification constantly formed in living organisms (Cohen et al. 2006) and typically further increased in animal- or plant-derived meals during storage or thermal processing (Goldberg et al. 2004). It is initiated by the reaction of reducing sugars, aldoses and ketoses, with protein amino groups (Yeboah et al. 1999) yielding imines that might undergo Amadori or Heyns rearrangements, respectively (Hodge 1955; Heyns and Noack 1962; Fig. 1). Under oxidative conditions, these Amadori and Heyns products are readily involved in further rearrangement and oxidative cleavage reactions yielding a heterogeneous group of so-called advanced glycation end-products (AGEs) (Grillo and Colombatto 2008; Fig. 1). Alternatively, AGEs can be formed by reaction of α -oxo-carbonyls with amino and guanidino groups in lysine and arginine residues (Ahmed et al. 1997, 2003; Fig. 1). The α -dicarbonyl compounds involved in these reactions (e.g. glyoxal and methylglyoxal) are generated by monosaccharide autoxidation (Wolff and Dean 1987), lipid peroxidation (Milic et al. 2013) or enzymes (Rabbani and Thornalley 2012). As AGEs are assumed to be toxic and pro-inflammatory in mammals, typically mediated by receptor-mediated NF- κ B activation (Schiekofer et al. 2003), their formation and degradation reactions need to be completely understood.

Though the mechanisms of α -dicarbonyl-mediated advanced glycation of lysine and arginine side chains were

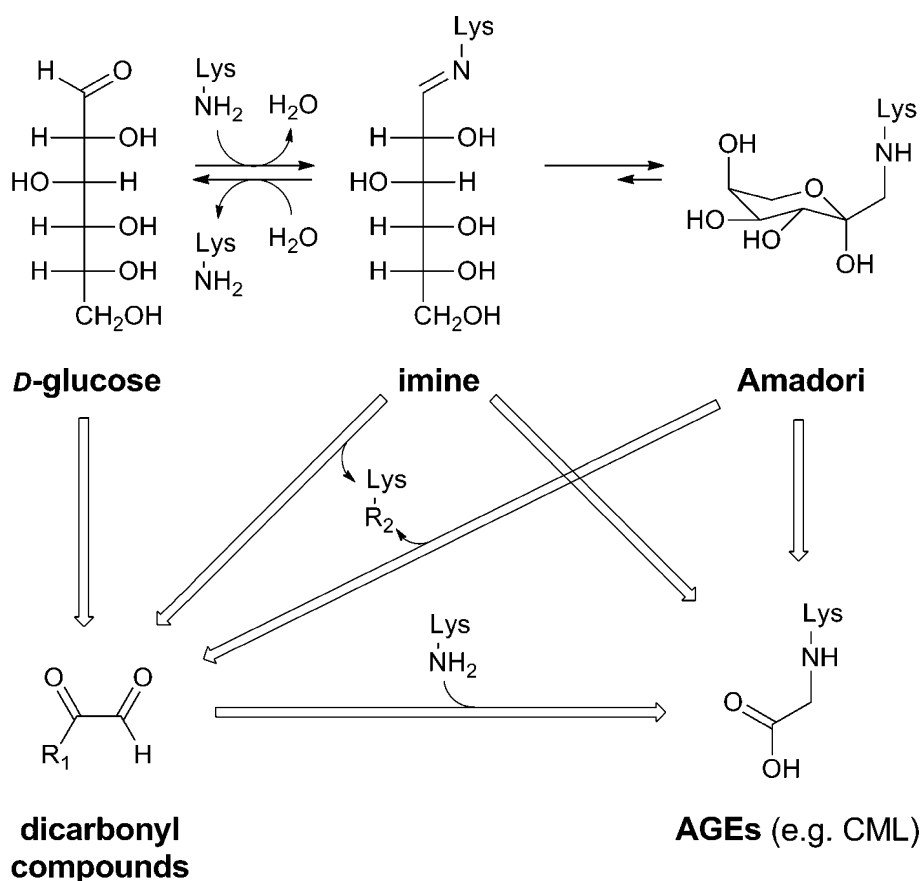
Handling Editor: F. Albericio.

Electronic supplementary material The online version of this article (doi:10.1007/s00726-015-1940-2) contains supplementary material, which is available to authorized users.

U. Greifenhagen · A. Frolov · R. Hoffmann (✉)
Faculty of Chemistry and Mineralogy, Institute of Bioanalytical
Chemistry, Universität Leipzig, Deutscher Platz 5,
04103 Leipzig, Germany
e-mail: hoffmann@chemie.uni-leipzig.de

U. Greifenhagen · A. Frolov · R. Hoffmann
Center for Biotechnology and Biomedicine, Universität Leipzig,
Deutscher Platz 5, 04103 Leipzig, Germany

Fig. 1 Lysine AGE formation pathways from glucose and Amadori compounds



comprehensively characterized for amino acids (Glomb and Monnier 1995; Kloepfer et al. 2011) and peptides (Frolov et al. 2014), AGE formation via degradation of Amadori and Heyns compounds is less understood. However, this aspect has a high relevance in physiology, food chemistry, and nutrition science. Indeed, Amadori compounds are produced during thermal processing of foods (Biemel et al. 2001; Meltretter et al. 2009; Schwietzke et al. 2011), while some foods, like milk, contain already significant glycation levels in the raw state (Ahmed et al. 2005; Meltretter et al. 2009). Although early glycation products do not appear to have physiological effects (Miyata and Sprague 1996), the sugar moieties can be involved in glycoxidation (Ahmed et al. 1986) or reversal of the Amadori rearrangement followed by the Namiki pathway (Hayashi and Namiki 1980) or autooxidation of the liberated sugar (Wolff and Dean 1987).

As glycated amino acids can be easily synthesized and their products reliably analyzed, Amadori degradation was comprehensively studied with purified N^α -fructosamines of various amino acids (Martins and Van Boekel 2003; Zhang et al. 2012) and N^α -protected lysyl N^ϵ -fructosamines (Zyzak et al. 1995; Akira and Hashimoto 2005). However, these convenient models do not resemble amino acid residues in proteins. On the other hand, protein models are too complex and difficult to interpret (Wells-Knecht et al. 1995). Thus, peptides represent

a good compromise (Jakas and Horvat 2003). Few years ago, we have established comprehensive methods to synthesize and purify glycated peptides (Frolov et al. 2006; Frolov and Hoffmann 2008), providing a convenient basis for Amadori degradation studies. This approach ensures adequate modeling of a ‘protein-like’ environment for a glycated lysyl residue (considering the denatured status of proteins during cooking), yielding limited number of degradation products that can be isolated and analyzed by mass spectrometry.

Here, we established an in vitro model to study thermal degradation of Amadori peptides, applied it to simulation of cooking processes, and comprehensively identified the resulting degradation products including the characterization of their formation kinetics. Moreover, we studied the effect of neighboring amino acid residues and reactive oxygen species (ROS) on the degradation of glycated peptides.

Materials and methods

Materials

Suppliers and their products were as follows: PolyPeptide Laboratories (Strasbourg, France): Fmoc-L-CML(O^tBu)(Boc)-OH (97.9 %); MoBiTec GmbH (Göttingen, Germany):

Fmoc-D/L-*ortho*- and Fmoc-D/L-*meta*-Tyr-OH (peptide synthesis grade); Iris Biotech GmbH (Marktredwitz, Germany): Fmoc-L-Arg(Pbf)-OH, Fmoc-L-Lys(formyl)-OH, Fmoc-rinkamide resin (peptide synthesis grade); ORPEGEN Pharma (Heidelberg, Germany): all other Fmoc-protected L-amino acids (peptide synthesis grade); Biosolve (Valkenswaard, Netherlands): *N,N*-dimethylformamide (DMF, ≥99.8 %), piperidine (≥99.5 %), dichloromethane (≥99.9 %); Carl Roth (Karlsruhe, Germany): trifluoroacetic acid (TFA, ≥99.9 %), acetic acid (100 %), α-D-glucose monohydrate (≥99.5 %); VWR International (Dresden, Germany): diethyl ether (100 %), acetonitrile (≥99.9 %). Sigma-Aldrich (Taufkirchen, Germany): acetic acid anhydride (≥99.9 %), di-*tert*-butyl dicarbonate (≥98.0 %), chloroform-D (≥99.8 atom-% D), diisopropylcarbodiimide (DIC, ≥98.0 %), ethyldiisopropylamine (DIPEA, ≥98.0 %), 1-hydroxybenzotriazole monohydrate (HOBt, ≥97 %), 2,3-*O*-isopropylidene-D-glyceric acid methyl ester (98 %), potassium hydroxide (≥90 %), 4-methylmorpholine (≥99.5 %), tetrakis(triphenylphosphine)palladium(0) (≥95 %), TFA (≥99.0 %) and heptafluorobutyric acid (HFBA, ≥99.5 %) as ion pair reagents, sodium hydrogen phosphate dihydrate (≥99.0 %), sodium dihydrogen phosphate dodecahydrate (≥99.0 %), iron(II) sulfate heptahydrate (≥99.0 %), diethylenetriamine pentaacetic acid (DTPA, ≥98 %), formic acid (mass spectrometry grade). Water was purified in-house (resistance 18 mΩ/cm) on a PureLab Ultra Analytic System (ELGA Lab Water, Celle, Germany).

Peptide synthesis

Sequences Ac-AKASAXFL-NH₂ with X = S (peptide 1), H (2), K (3), R (4), D (5), and E (6) were synthesized on a Syro2000 multiple peptide synthesizer (MultiSynTech GmbH, Witten, Germany) by 9-fluorenylmethoxycarbonyl/*tert*-butyl (Fmoc/*t*Bu)-chemistry using 8 equivalents (eq.) of Fmoc-amino acid derivatives activated with DIC/HOBt in situ (Frolov et al. 2006). Lysine residues to be glycosylated were incorporated as Fmoc-N^ε-(allyloxycarbonyl)lysine (Fmoc-K(Alloc)-OH). Following N-terminal acetylation (Ac), the allyloxycarbonyl (Alloc) group was selectively removed (Dangles et al. 1987). Glycation was performed on solid phase (1 mg peptidyl resin) with α-D-glucose monohydrate in DMF (0.25 mol/L, 0.2 mL) at 120 °C for 75 min (peptides 1, 3, 5, and 6) or at 115 °C for 40 min (peptides 2 and 4) (Frolov et al. 2006). All peptides were purified by ion pair reversed-phase high-performance liquid chromatography (IP-RP-HPLC) using a Jupiter C₁₈-column (Phenomenex Ltd., Aschaffenburg, Germany) with aqueous acetonitrile gradients containing 0.1 % (v/v) TFA or 0.1 % (v/v) HFBA as ion pair reagents for non-glycosylated and Amadori-modified peptides (Frolov and Hoffmann 2008), respectively. Authentic standard peptides were prepared as described in Protocol S1.

Peptide incubation

Dried peptide aliquots [24 nmol, in 0.5 mL Eppendorf safe lock tubes (Eppendorf AG, Hamburg, Germany)] were dissolved in sodium phosphate buffer (50 μL, 100 mmol/L, pH 7.4) without any additives or containing (1) 18 μmol/L iron(II) sulfate, (2) 590 μmol/L iron(II) sulfate, (3) 18 μmol/L iron(II) sulfate and 60 μmol/L ascorbic acid, or (4) 590 μmol/L iron(II) sulfate and 1.2 mmol/L ascorbic acid. Samples were incubated at 95 °C for 0, 5, 10, 15, 30, 60, and 240 min in triplicates, while continuously shaking at 450 rpm. The reactions were stopped by cooling on ice, centrifugation (12.0×g, 15 s), and addition of aqueous DTPA (6 mmol/L, 10 μL). Samples were stored at −80 °C. Prior to their first analysis, the samples were dried at room temperature under reduced pressure and reconstituted by addition of acetonitrile (7.5 μL) and a mixture of formic acid [0.1 % (v/v)] and acetonitrile [1 % (v/v)] in water (52.5 μL). Control samples with the non-glycosylated peptides were always treated in parallel under the same conditions.

Mass spectrometry

The degradation mixture (250 pmol) was separated on HPLC (1100 system, Agilent Technologies, Böblingen, Germany) using an Aqua C₁₈-column (length: 150 mm, inner diameter: 2.0 mm, particle size: 3 μm, pore size: 125 Å) with a flow rate of 0.22 mL/min. Elution was achieved by isocratic conditions 3 % eluent B for 5 min, followed by two linear gradients to 40 % B (23 min) and 95 % B (3 min) using water (eluent A) and acetonitrile (eluent B) containing each formic acid [0.1 % (v/v)]. The eluate was transferred on-line to an QqTOF-MS (QSTAR Pulsar I, AB Sciex, Darmstadt, Germany) equipped with a TurboIon source, operated in positive ion mode, and controlled by Analyst QS 1.0 software (AB Sciex). Operating parameters and compositions of mass calibration solutions are given in Table S1. Analytes were quantified by integration of the corresponding extracted ion chromatograms (XICs, $m/z_{\text{obs}} \pm 0.10 m/z$ units, smoothing factor: 3) and normalization to the highest average value in the kinetics. Theoretical m/z values for peptide (fragment) ions were calculated using the Bioanalyst QS 1.0 software package.

Mass spectra were additionally acquired on a LTQ-Orbitrap XL ETD MS (Thermo Fischer Scientific GmbH, Bremen, Germany) due to its higher mass accuracy to determine the elemental composition of the analytes. Fractions of varied volume were collected manually from the RP-HPLC (see above), dried, and reconstituted in a mixture of acetonitrile [50 % (v/v)], methanol [25 % (v/v)], and acetic acid [1 % (v/v)] in water (50 μL). The peptide solutions were electrosprayed by a nanoflow ion source (TriVersa NanoMate, Advion BioSciences, Ithaca, NY, USA) using

Table 1 Sequences and analytical parameters of all compounds identified in the degradation experiments of peptide I_{Am}

Peptide	Sequence/structure	[M+H] ⁺		Modification-associated mass shift _{calc} [Da]	t_R [min]
		m/z_{exp}	m/z_{calc}		
I_{Am}	Ac-A-[N ^ε -(fructosyl)lysine]-ASASFL-NH ₂ ^a	997.50	997.5201	+162.0529	25.0
I	Ac-AKASASFL-NH ₂ ^a	835.45	835.4672	–	25.1
I_{cm}	Ac-A-[N ^ε -(carboxymethyl)lysine]-ASASFL-NH ₂ ^a	893.46	893.4727	+58.0055	26.0
$I_{ethanallyl}$	Ac-A-[N ^ε -(ethanallyl)lysine]-ASASFL-NH ₂	877.47	877.4778	+42.0106	25.3
$I_{glycerinyl}$	Ac-A-[N ^ε -(glycerinyl)lysine]-ASASFL-NH ₂ ^a	923.47	923.4833	+88.0161	27.0
I_{acetyl}	Ac-A-[N ^ε -(acetyl)lysine]-ASASFL-NH ₂ ^a	877.45	877.4778	+42.0106	28.0
I_{formyl}	Ac-A-[N ^ε -(formyl)lysine]-ASASFL-NH ₂ ^a	863.42	863.4621	+27.9949	27.6
I_{methyl}	Ac-A-[N ^ε -(methyl)lysine]-ASASFL-NH ₂	849.45	849.4829	+14.0157	25.5
$I_{formate}$	Ac-A-[N ^ε -(formate)lysine]-ASASFL-NH ₂	879.42	879.4571	+43.9899	27.3
$I_{allysine}$	Ac-A-allysine-ASASFL-NH ₂	834.45	834.4356	–1.0316	27.9
$I_{allysine+62}$	Ac-AK ₋₁ ASASFL(62)	879.41	–	–	27.9
$I_{allysine+16}$	Ac-(AK ₋₁) ₊₁₆ ASASFL-NH ₂	850.37	–	–	27.8
I_{Ypara}	Ac-AKASASY _{para} L-NH ₂ ^a	851.46	851.4621	+15.9949	22.5
I_{Ymeta}	Ac-AKASASY _{meta} L-NH ₂ ^a	851.46	851.4621	+15.9949	23.4
I_{Yortho}	Ac-AKASASY _{ortho} L-NH ₂ ^a	851.46	851.4621	+15.9949	26.5
$I_{cmYpara}$	Ac-A-[N ^ε -(carboxymethyl)lysine]-ASASY _{para} L-NH ₂ ^a	909.43	909.4676	+58.0055, +15.9949	23.6
$I_{cmYmeta}$	Ac-A-[N ^ε -(carboxymethyl)lysine]-ASASY _{meta} L-NH ₂	909.43	909.4676	+58.0055, +15.9949	24.3
$I_{cmYortho}$	Ac-A-[N ^ε -(carboxymethyl)lysine]-ASASY _{ortho} L-NH ₂	909.43	909.4676	+58.0055, +15.9949	27.5
$I_{fragment1}$	H-ASASFL-NH ₂ ^a	594.30	594.3246	–	23.9
$I_{fragment2}$	H-SASFL-NH ₂ ^a	523.26	523.2875	–	23.6
$I_{fragment3}$	Ac-AKASAS-NH ₂ ^a	575.28	575.3148	–	3.2

^a Synthesized authentic standard peptides possess the same t_R , m/z , and MS/MS characteristics

nano electrospray chips (1.5 kV ionization voltage, 1.3 psi backpressure) into a LTQ-Orbitrap XL ETD MS. The temperature of the transfer capillary was set to 200 °C and the tube lens voltage to 115 V. Mass spectra were recorded from m/z 400 to 2000 in the orbitrap mass analyzer (resolution: 60,000 at m/z 400). Tandem mass spectra were acquired by performing CID (isolation width 2 u, normalized collision energy 35 %, activation time 30 ms, activation Q 0.25) in the linear ion trap. Data were analyzed by using Xcalibur software (version 2.0.7).

RP-HPLC

The samples of peptides ($I-6$)_{Am} incubated for 0 and 4 h (5 µg peptide mixture) were separated by the gradient described above (section 2.4), but using a Beckmann System Gold HPLC system (507e autosampler, 125 solvent system, 166 detector) controlled by 32Karat 7.0 software (all Beckman-Coulter, Krefeld, Germany), and the absorbance was recorded at 214 nm. The corresponding non-glycated control peptide (1 µg) was analyzed immediately after the incubation samples to confirm the retention times. Peak integration parameters were: width 0.3 and threshold 10,000. Relative product quantities were calculated by

dividing the peak area of the products (4 h) by that of the starting material (0 h) to normalize the peak areas obtained by LC-MS.

Statistical analysis

Calculations were performed with Excel 2003 software (Microsoft) using the implemented average and standard deviation functions. Statistical significance was determined in the same program with a two-tailed t test. All data are presented as average ± standard deviation ($n = 3$).

Results

Identification and characterization of Amadori degradation products

Amadori and unmodified peptides incubated in parallel were analyzed with RP-HPLC-ESI-QqTOF-MS, and products were characterized with MS/MS (Table 1, Table S2, S3, S4, S5, Fig. 2, Fig. S1, S2). The total ion current and the absorbance chromatograms of the incubated Amadori peptide I_{Am} were dominated by peaks corresponding to the deglycated

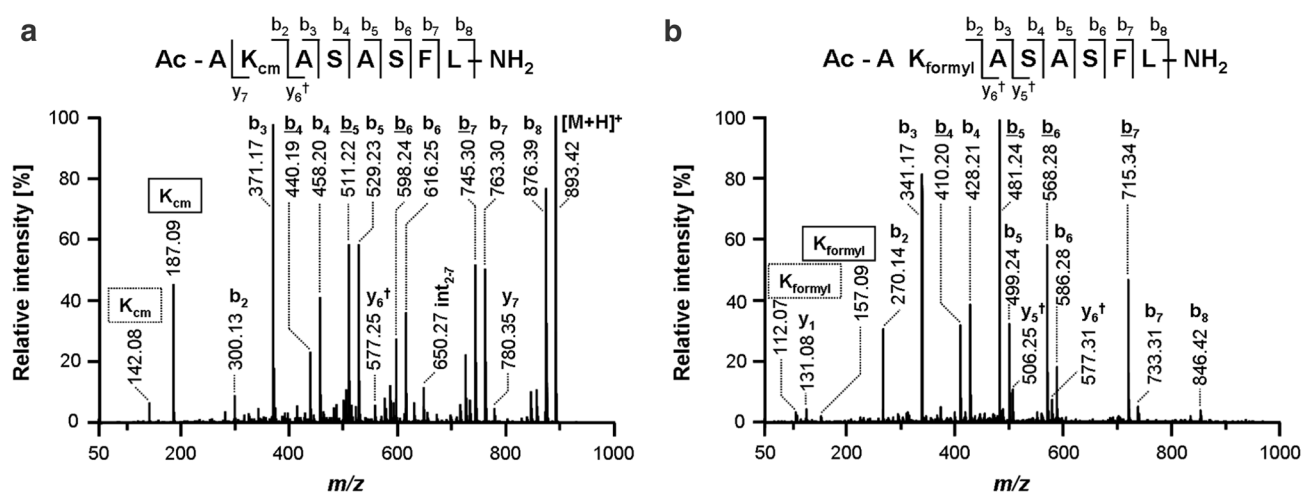


Fig. 2 Product ion spectra of *I*_{cm} (a) and *I*_{formyl} (b) acquired on a QSTAR Pulsar I instrument (AB Sciex). Fragment ions formed by loss of H₂O (underlined) or NH₃ ([†]) were observed. α -Amino- ϵ -

caprolactam-derived ions are **boldly**, tetrahydropyridine-derived ions are framed with dots. *Internal ions* are denoted as int_{a-b} with a and b being the terminal residues

(unmodified) (*m/z* 835.45, *I*, Fig. 3a) and the CML-containing peptide (*m/z* 893.46, *I*_{cm}, Fig. 3b). Six further peptide products modified on lysine contained sugar-derived modifications: *N*^ε-(ethanallyl)lysine (*m/z* 877.47, *I*_{ethanallyl}, Fig. 3c), *N*^ε-(glycerinyl)lysine (*m/z* 923.47, *I*_{glycerinyl}, Fig. 3d), *N*^ε-(acetyl)lysine (*m/z* 877.45, *I*_{acetyl}, Fig. 3e), *N*^ε-(formyl)lysine (*m/z* 863.42, *I*_{formyl}, Fig. 3f), and *N*^ε-(methyl)lysine (*m/z* 849.39, *I*_{methyl}, Fig. 3g). Another product with a mass increase of 44 Da at the lysyl residue was annotated as *N*^ε-(formate)lysine (*m/z* 879.44, *I*_{formate}, Fig. 3h). Two peptides contained α -amino adipic semialdehyde (hereafter termed allysine), which is derived from oxidation of the lysine side chain, in an otherwise unmodified peptide (*m/z* 834.45, *I*_{allysine}, Fig. 3i), and in a peptide carrying an unknown C-terminal modification of 62 Da (*m/z* 879.41, *I*_{allysine+62}). Finally, a peptide with an overall mass shift of +15 Da to the unmodified peptide (*m/z* 850.37, *I*_{allysine+16}) was detected, which displayed a neutral loss of 16 *m/z* units at residues 1 or 2 yielding presumable allysine (−1 Da) structure (Fig. S1f). This loss excludes α -amino adipic acid from the putative structures, as carboxylic acids are not prone to oxygen loss in collision-induced dissociation fragmentation. Not only the lysine residue, but also the phenylalanine residue was oxidized yielding *ortho*- (*I*_{Yortho}), *meta*- (*I*_{Ymeta}), and *para*-tyrosine (*I*_{Ypara}) (*m/z* 851.46, Fig. 3j), respectively. A combination of these oxidation- and sugar-derived modifications was observed in peptides *I*_{cmYortho}, *I*_{cmYmeta}, and *I*_{cmYpara} (*m/z* 909.43). In addition to these products containing the intact peptide backbone, peptide fragments containing only the six (*I*_{fragment1}) or five C-terminal (*I*_{fragment2}) or the six N-terminal amino acid residues (*I*_{fragment3}) were identified. These were the only products formed in comparable amounts in the control incubations containing the

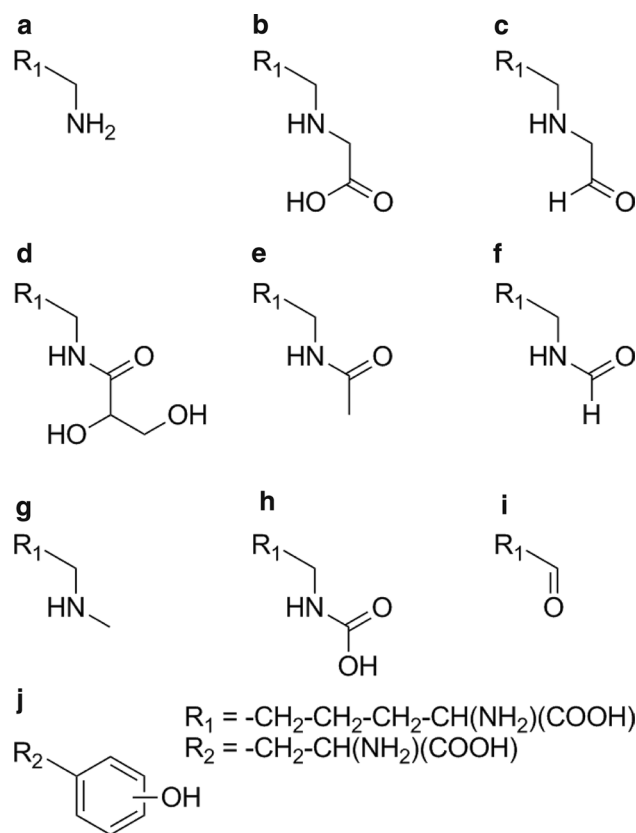
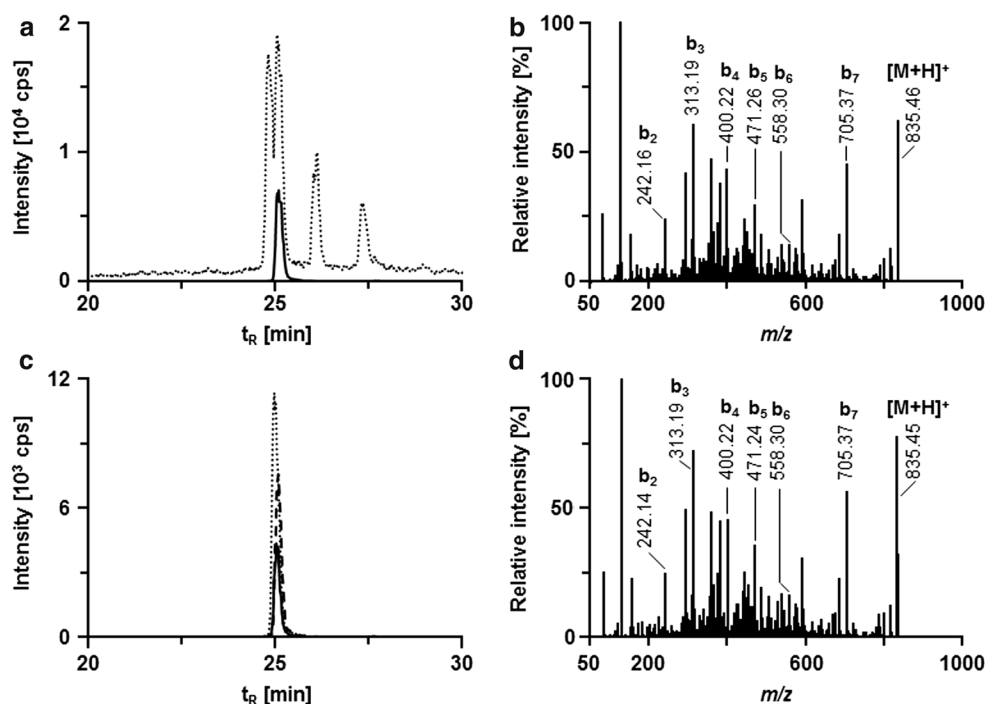


Fig. 3 Amino acid-based side chain structures of *I*_{Am} degradation products: *I* (a), *I*_{cm} (b), *I*_{ethanallyl} (c), *I*_{glycerinyl} (d), *I*_{acetyl} (e), *I*_{formyl} (f), *I*_{methyl} (g), *I*_{formate} (h), *I*_{allysine} (i), *I*_{Yortho}, *I*_{Ymeta}, or *I*_{Ypara} (j), respectively

unmodified peptide *I*. Further oxidation products, derived by, e.g., dihydroxylation on the phenylalanine residue or bityrosine formation, were not detected.

Fig. 4 Identification of *I* as a product of I_{Am} degradation at 95 °C and high-iron condition for 5 min. The total ion chromatogram (dotted curve) of the RP-HPLC–MS analysis was extracted for the m/z of *I* (835.44 ± 0.1 Da, solid line) (a). An RP-HPLC–MS/MS analysis fragmenting *I* yielded the product ion spectrum shown in (b). Coelution of *I* present in the incubation sample (dashed), as synthetic authentic standard peptide (solid), and the incubation sample spiked with the same amount of standard peptide (dotted) is shown by overlay of the XICs (c). Additionally, the authentic standard peptide yielded a principally identical tandem mass spectrum (d, further details in Table S4)



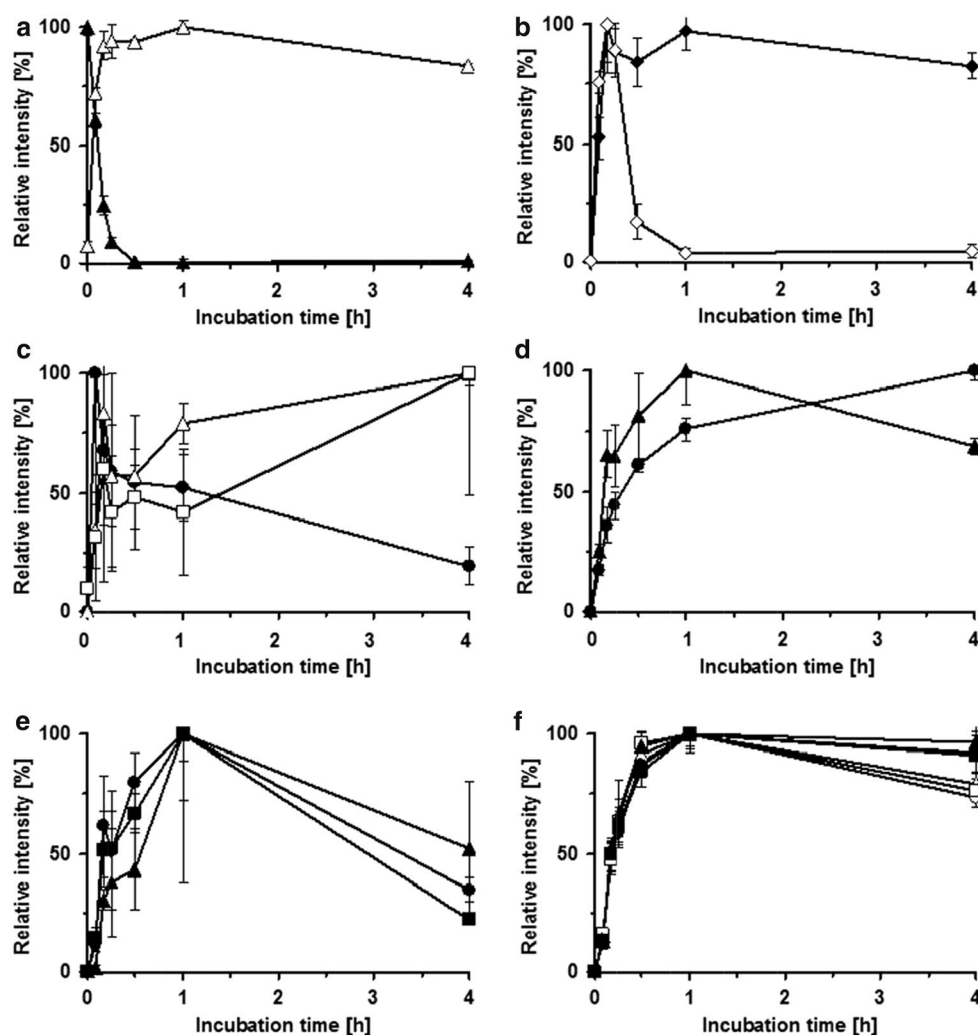
Twelve of the structures described above were eventually confirmed by their coelution with synthetic peptides and characteristic fragmentation patterns (Table S2, S3, S4, Fig. 4). All other signals were annotated by exact mass and fragmentation pattern (Table S5, Fig. S1).

Kinetics of Amadori degradation and product formation

The identified degradation products (Table 1) were quantified relative to the highest peak area observed using a window of 0.10 m/z units (Fig. 5). The Amadori peptide was degraded within 15 min to <10 % of its original content and completely after 30 min (Fig. 5a). The products formed could be grouped by their fast or slow kinetic formation rates. The deglycated peptide *I* (Fig. 5a) appeared with the fastest rate reaching already 70 % of its steady-state value after 5 min accounting for approximately 40 % of the Amadori peptide loss based on the UV peak area ratio relative to I_{Am} . Formation rate of I_{cm} was similar (51 %, 5 min) and remained constant after reaching the maximum value ($p > 0.05$, Fig. 5b). Peptide $I_{ethanoyl}$ was detected with highest intensity after 5 min and degraded rapidly until 10 min. Interestingly, its degradation was slower than its formation. The kinetics of the amide-AGEs were less obvious (Fig. 5c). The large standard deviations observed here resulted from their low signal intensities, which could be attributed to their low concentrations, low ionization efficiencies, or their complex formation and degradation pathways. Therefore, no significant differences between early time points (5–30 min) and the last

time point (4 h) were observed in the peak areas of both $I_{glycerinyl}$ and I_{acetyl} , whereas that of I_{formyl} increased steadily, even though significant differences were only observed from 0.5 to 4 h. Products I_{methyl} and $I_{formate}$ were formed over a longer period than *I* and I_{cm} , reaching their half-maximum levels between 10 and 15 min (Fig. 5d). The peak area corresponding to I_{methyl} increased over the whole period, suggesting that it is constantly formed or that its formation rate exceeds its degradation, whereas $I_{formate}$ decreased from 1 to 4 h by 30 %. Oxidation on the lysine side chain yielding $I_{allysine}$ occurred slower than CML formation (≈ 48 %, 10 min, Fig. 5e), peaked at 1 h, and decreased afterward to approximately one-fifth of its maximum level indicating consecutive degradation. The two related products with unknown structures $I_{allysine+62}$ and $I_{allysine+16}$ (Fig. 5e) comprising the allysine residue principally followed the same kinetics, which suggests the oxidation of the lysyl residue as the rate-limiting step. Hydroxylation of the phenylalanine residues was principally independent of the hydroxylation position and slower than the CML and allysine formation (41–45 %, 15 min, Fig. 5f). Consequently, the rate-limiting step in the formation of I_{cmY} (Fig. 5f) was the hydroxylation, which is reflected by its formation kinetics following closely I_Y and not I_{cm} . The slowest reaction observed was the degradation of the peptide backbone ($I_{fragment1}$, $I_{fragment2}$, Fig. S3), reaching their half-maximal intensities at approximately 30 min, which were independent of glycation as the same kinetics were observed for the unmodified control peptide (Fig. S3).

Fig. 5 Kinetics of Amadori peptide degradation (I_{Am} , filled triangle, **a**) and formation of products I (triangle, **a**), I_{cm} (filled diamond, **b**), $I_{ethanalyl}$ (diamond, **b**), amide AGE-containing peptides (glycerinyl, filled circle, acetyl, square, and formyl lysine, triangle, all in **c**), $I_{formate}$ (filled triangle, **d**), I_{methyl} (filled circle, **d**), peptides containing allysine and related structures ($I_{allysine}$: filled square, $I_{allysine+62}$: filled circle, $I_{allysine+16}$: filled triangle; all in **e**), and peptides containing *para*- (triangle), *meta*- (square), and *ortho*-tyrosine (circle) with unmodified lysine or CML (filled symbols, all **f**). Plotted are integrated XICs (average \pm standard deviation, $n = 3$) that were normalized to the highest average value obtained for each analyte

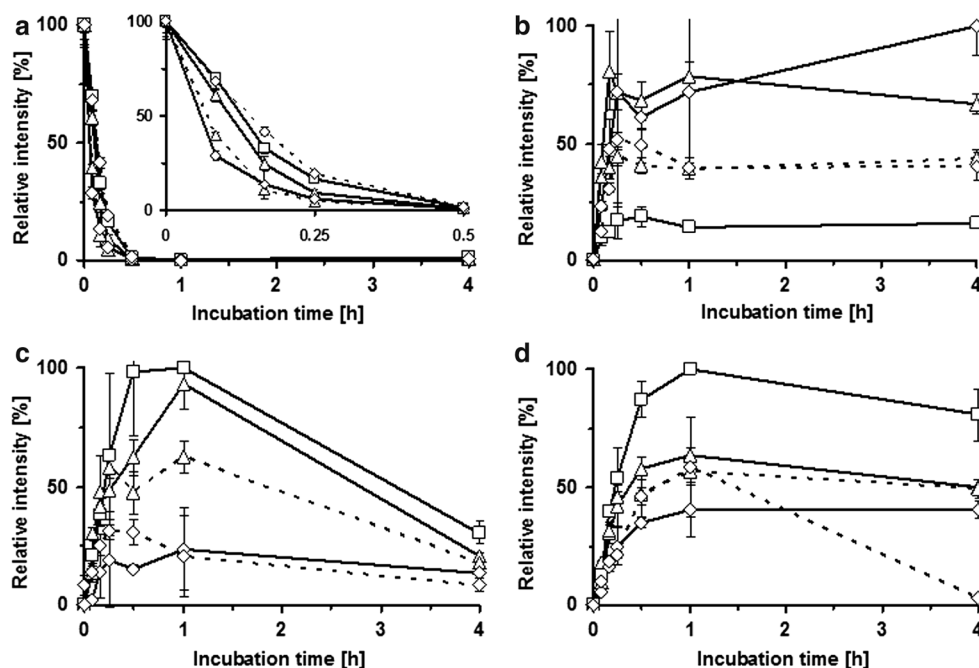


ROS-dependence of Amadori degradation and product formation

As Amadori products are mostly degraded by oxidation, we incubated peptide I_{Am} next in the absence (*iron absence*) or presence of 18 and 590 $\mu\text{mol/L}$ iron(II) (*low* and *high iron*), which are known to produce ROS. Additionally, combinations of iron(II) and ascorbic acid concentrations were used: 18 $\mu\text{mol/L}$ iron(II) with 60 $\mu\text{mol/L}$ ascorbic acid (*low iron/ascorbate*) and 590 $\mu\text{mol/L}$ iron(II) with 1.2 mmol/L ascorbic acid (*high iron/ascorbate*). The low iron and ascorbic acid concentrations resemble human plasma (Statland et al. 1976; Simon and Hudes 1999) and the higher concentrations were chosen according to the peptide/iron(II)/ascorbic acid ratio shown most effectively oxidizing peptides (Bollineni et al. 2011). The Amadori peptide degradation was always completed within 30 min regardless of the reaction conditions, similar to the buffer condition described above. Compared to the *low-iron* condition, the degradation of the Amadori peptide was slightly enhanced under *high iron* and

low iron/ascorbate conditions, whereas *high iron/ascorbate* decelerated the degradation to the level of phosphate buffer (Fig. 6a). The difference was most obvious after 10 min, where the *high iron/ascorbate* conditions showed the lowest degradation. The *low*- and *high-iron* conditions initiating fast degradation of the Amadori peptide were also the most effective in CML peptide production yielding 100 and 67 % of its maximum value compared to only 16 % in buffer (Fig. 6b). This observation is unbiased for potentially different oxidation amounts occurring in parallel at other residues, as the formation of I_{cmY} follows a similar pattern (Fig. S4 g–i). Contrary to I_{cm} , $I_{allysine}$ (Fig. 6c), and I_{Ypara} (Fig. 6d) were formed in maximum amounts in the absence of iron(II) with $I_{allysine}$ reaching its maximum after 60 min under all conditions except *high iron/ascorbate* that peaked between 15 and 30 min. Thus, $I_{allysine}$ was produced most when iron was absent or of low concentration, and decreased with addition of ascorbate to medium (*low iron/ascorbate*) or low levels (*high iron/ascorbate*). In contrast to instable $I_{allysine}$, the *para*-Tyr modification appeared to

Fig. 6 Degradation of Amadori peptide I_{Am} (a) and formation of the CML- (I_{cm} , b), allysine- ($I_{allysine}$, c), and *para*-tyrosine-containing peptide (I_{Ypara} , d) in phosphate buffer (pH 7.4) in iron absence (square), or in the presence of low (triangle) or high iron (diamond) with (dots) or without ascorbate (lines), respectively



be stable (Fig. 6d), as its content increased always during the first hour and was stable afterward except for *high iron/ascorbate* where it decreased by more than 95 % (4 h) from its maximum after 1 h.

Influence of neighbored residues on Amadori degradation and product formation

The influence of position $i + 4$ relative to the glycation site was studied with sequences Ac-AK_{Am}ASAXFL-NH₂ relative to the neutral serine ($X = S$, I_{Am}), as in the experiments described above, for basic [$X = H$ (2_{Am}), K (3_{Am}), and R (4_{Am})] or acidic residues [D (5_{Am}) and E (6_{Am})]. These peptides were incubated under *low iron* condition. As the ionization efficiencies of the different products might vary, the peak areas were normalized to the peak areas obtained by UV absorbance in RP-HPLC. The two main products, i.e., the deglycated and CML-containing peptides were relatively quantified by dividing their UV peak areas at 4 h by the Amadori peptide UV peak areas of the untreated sample (0 h) and normalizing the peak areas of the corresponding XICs. Based on these normalized values, the whole kinetic curves of the deglycated and CML-containing peptides were reconstructed in entities of relative product amounts (Fig. 7). Analytical parameters of (2–6)_{Am} and their main products are summarized in Table S6 and Fig. S2.

Degradation of the Amadori peptide was enhanced by basic residues in position $i + 4$ (Fig. 7a), with Lys and Arg showing the most pronounced effect. Acidic residues had no (Glu) or only slight delaying effects (Asp). Interestingly, faster degradation rates did not lead to higher yields in

deglycated (Fig. 7b) or CML-containing peptides (Fig. 7c). In contrast, peptides 5 and 6 were significantly more abundant after 4 h than peptide 1 ($p < 0.01$). Although the degradation of peptides 3_{Am} and 4_{Am} showed only small, but significant differences (1 vs. 2 % at 15 min, $p < 0.01$), the yield of their corresponding deglycated products showed a well-perceivable difference (13 vs. 17 % at 4 h, $p < 0.01$). 5_{Am} was transformed by 29 ± 1 % to the CML-product, whereas the other sequences yielded only 13–23 %. Interestingly, the formation kinetics of deglycated and CML-containing peptides showed reduced peptide contents after 15 or 30 min, which was in both cases most obvious for peptide 6, but occurred also for the other sequences.

Discussion

The degradation of *N*^ε-fructosyl lysine was studied with Amadori peptide Ac-AK_{Am}ASASFL-NH₂ (I_{Am}) at 95 °C. N-terminal acetylation and C-terminal amidation were chosen to limit the reactive groups to the modified lysine besides oxidation of phenylalanine. Thus, products from three principal reaction pathways were expected: (1) sugar-related modifications on the lysine side chain resulting from the degrading sugar moiety or the reaction with monosaccharide autooxidation products of released sugars and dicarbonyls, products formed by (2) oxidation of lysine and phenylalanine residues, and (3) cleavage of the peptide backbone.

The Amadori peptide (I_{Am}) degraded to <10 % within 15 min and quantitatively after 30 min (Fig. 5a) which is

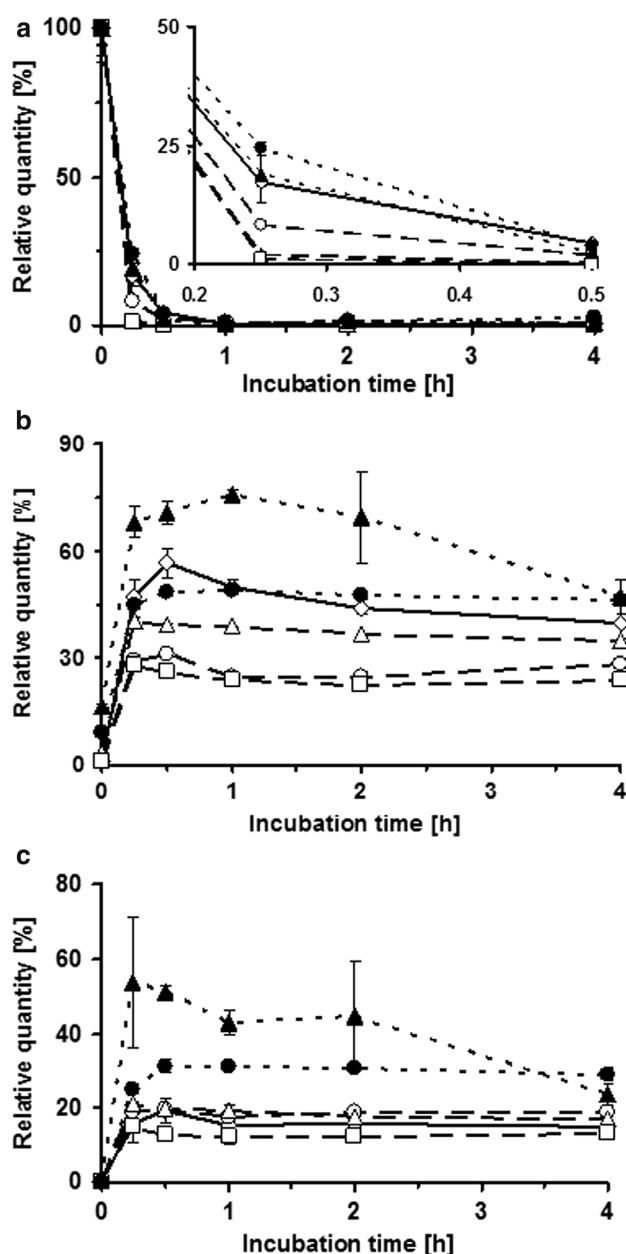


Fig. 7 Degradation kinetics of Amadori peptides Ac-AK_{Am} ASAXFL-NH₂ with X = S (*I*_{Am}, diamond), H (*2*_{Am}, circle), K (*3*_{Am}, square), R (*4*_{Am}, triangle), E (*5*_{Am}, filled triangle), and D (*6*_{Am}, filled circle) in 100 mmol/L phosphate buffer containing 18 μmol/L iron(II) at 95 °C (a). These reactions mainly produced the deglycated peptides (b) and the CML-containing peptides (c)

significantly faster than reported for *N*-glycated amino acids. For example, 5 % or more of *N*-(1-deoxy-D-fructos-1-yl)glycine remained when incubated at 90–100 °C for 1.5 h (Staempfli et al. 1994; Davidek et al. 2002; Martins et al. 2003). *N*-terminally glycated peptides were studied only up to 70 °C, but showed an even slower degradation behavior (Jakas and Horvat 2003), which could be attributed to either the lower temperature and the lower

concentration of catalytically active phosphate buffer or their generally higher stability. Thus, our studies indicate a substantially lower stability of ϵ -*N*-Amadori modifications at the peptide level. The degradation pace of the Amadori moiety varies with the concentrations of iron(II) and ascorbic acid (Fig. 6a) indicating that the degradation of the Amadori peptide does not only take place via metal ion-independent release of the intact sugar via reverse Amadori rearrangement but as well due to oxidative degradation of the peptide-bound sugar. Unexpectedly, the *high iron/ascorbate* condition showed the slowest Amadori degradation, although ascorbic acid was added to reduce iron(III) for regenerating iron(II) and thus to enhance ROS production. However, ascorbic acid may act additionally as anti-oxidant by capturing and deactivating radicals. This dual nature is concentration dependent (Buettner and Jurkiewicz 1996), and the *high ascorbate* condition seems to be sufficiently high to display anti-oxidant effects.

The degradation of the Amadori peptide yielded dominantly the unmodified and the CML-containing peptide accounting for 40 and 15 % of the Amadori peptide loss, respectively, whereas the aforementioned studies with *N*-(1-deoxy-D-fructos-1-yl)glycine (Davidek et al. 2002; Martins et al. 2003) noted 60–80 % unmodified amino acid. The lower yields of unmodified peptides may be explained by modifications of other residues, such as hydroxylation of phenylalanine. However, these products were formed in relatively low quantities and thus contributed only minimally to the lack. More likely, this difference is attributed to CML, a modification that has been reported to occur on α -amino groups (Cai and Hurst 1999), but might occur to a significantly lower degree at the *N*^α compared to the *N*^ε position. The summed yields of CML- and unmodified lysine-containing peptide (55 %) do indeed closely resemble the yields at the amino acid level (Davidek et al. 2002). Furthermore, peptides *I*_{cm} and *I* were also formed the fastest among all products observed (Fig. 5a, b), indicating that these products are formed directly from the Amadori-modified peptide. While this is accepted for the reverse Amadori rearrangement (and subsequent hydrolysis), the reactions leading to CML are still in discussion. Glyoxal—a dicarbonyl compound formed during saccharide autoxidation—reacts with amine groups to form an imine yielding after subsequent redox reactions CML (Glomb and Monnier 1995). CML formation via saccharide autoxidation products has been termed ‘autoxidative glycosylation’ (Wolff and Dean 1987). Alternatively, Amadori products may form CML by keto–enol tautomerism, retro–aldol cleavages, and oxidative steps without dealkylation of the amine (‘glycoxidation’) (Ahmed et al. 1986). Hydroxylation of Phe is a radical reaction (Dorfman and Adams 1973) and is therefore suitable to trace the short-lived hydroxyl radicals produced during hexose

oxidation. As hydroxylation was much slower than CML formation, the ‘autoxidative glycosylation’ contributes most likely only in minor fashion to CML formation. Moreover, degradation experiments with 3_{Am} and 4_{Am} , comprising lysine or arginine, respectively, revealed only one carboxymethylated peptide-containing CML in position 2 and not at position 6 (Fig. S2f+i). This is in accordance with experiments on the protein level performed at 37 °C (Brock et al. 2003). Additionally, we observed a peptide with a +42 Da-increment on the Lys position that showed an intermediate behavior with a similar formation rate as the CML-containing peptide (Fig. 5b). As the acetylated peptide (I_{acetyl}) eluted later, we suppose an ethanallyl group ($I_{ethanallyl}$). Though this structure can be formed by the reaction of glyoxal with the N^6 -amino group, the resulting Schiff base had to be reduced, which appears unlikely under oxidative conditions. Instead, $I_{ethanallyl}$ could be formed via retro-aldol reaction cleaving the sugar between C2 and C3 after a keto-enol tautomerism on the Amadori compound till C4 which is possible (Biemel et al. 2002). In this respect, $I_{ethanallyl}$ supports CML formation via ‘glycooxidation’ of the Amadori modification.

Besides CML as the most abundant AGE, the ‘amide-AGEs’ I_{acetyl} , $I_{glycerinyl}$, and I_{formyl} were detected in agreement with studies on N^{α} -Boc-lysine (Smuda et al. 2010) and in case of the formylation also at the protein level (Hasenkopf et al. 2002). On the amino acid level, <0.15 % of the 1-deoxyglucosone deployed was transferred to an amide AGE at 37 °C (Smuda et al. 2010). 1-Deoxyglucosone was produced during *N*-(1-deoxy-D-fructos-1-yl)glycine degradation (100 °C) by <1% (Martins et al. 2003). Thus, the detection of 1-deoxyglucosone-derived amide-AGEs at very low degrees was expected.

Additionally to the sugar-derived modifications, several products of oxidative damage to the peptide were observed. Their amounts decreased in the order *iron absence* > *low iron* > *high iron* (Fig. 6 and Fig. S4), which is in contrast to the group of sugar-related modifications that increased with iron(II) concentration. As both modification types need an oxidative environment for their formation, a possible explanation has to consider the concentration of ROS and the concurrence of parallel reaction pathways. Thus, the degradation of the sugar backbone might be possible in various pathways with only distinct products able to form AGEs via ROS-dependent pathways. Higher ROS concentrations would enhance these pathways and thus produce more AGEs from a limited sugar amount. In this context, the ROS-dependent quantities of I_{cmY} , combining AGE- and oxidative modification, have to be considered (Fig. S4 g–i). While the hydroxylation of the phenylalanine is rate limiting, the pattern resembles I_{cm} indicating the hydroxylation to occur at a constant percentage of the CML-containing peptide.

Alternatively, it could be assumed that the products of oxidative damage presented here are ‘moderately oxidized,’ whereas ‘strongly oxidized’ products (e.g. bityrosine formation, combination of different oxidation patterns) remained below the limit of detection. In that respect, the higher abundance of ‘moderately oxidized’ products under conditions with lower ROS concentration seems comprehensible. For example, the isomeric Tyr-containing peptides (I_{Yortho} , I_{Ymeta} , I_{Ypara}) are formed via addition of hydroxyl radicals (Dorfman and Adams 1973) and could be considered as products of ‘moderate oxidation.’ The fact that they were not observed in control incubations without ascorbic acid emphasizes the oxidative stress caused by the degrading Amadori moiety. Interestingly, the quantities of I_{Yortho} , I_{Ymeta} , and I_{Ypara} differ only slightly between 1 and 4 h, except for the *high iron/ascorbate* condition (Fig. 6d and S4 e–f). There, a pronounced decrease (I_{Yortho}) or almost complete disappearance (I_{Ypara} , I_{Ymeta}) was observed, which could indicate further oxidation to occur. Assuming that the oxidative damage observed results from ‘moderate’ oxidations, peptide cleavage should not result from oxidation (Stadtman 1993), but rather from hydrolysis at labile peptide bonds (Han et al. 1983; Kahne and Still 1988). Thus, peptide cleavage would occur independently from the radical-providing sugar moiety, which explains the fact that peptide fragments, but not the tyrosine-containing peptides were produced in significant amounts in the control incubations (Fig. S3). Similarly, $I_{allysine}$ formation was suggested to be radical dependent (Stadtman 1993) and occurred here exclusively in the presence of the degrading Amadori modification (Fig. 5e). The observation of $I_{allysine}$ is important, as this modification has been observed in glycation systems on the protein level (Akagawa et al. 2005; Meltretter and Pischetsrieder 2008) and thus validates the peptide model. The allysine residue was identified as a single modification ($I_{allysine}$) and in combination with an unknown modification at the C-terminus ($I_{allysine+62}$) and residue 1 or 2 ($I_{allysine+16}$). All show very similar instable kinetics and ROS-dependent behavior (Fig. 5e and S4 c–d), indicating that the allysine is rate limiting for their formation and less stable than the second modification.

Previous studies indicate different lysine reactivities in glycation, depending on neighboring residues affecting the pK_a of lysine, or acting in local catalysis either directly or via their ability to bind catalytically active phosphate (Zhang et al. 2011). For example, aspartatic and glutamatic acids are overrepresented near ‘reactive’ lysines (Watkins et al. 1985; Zhang et al. 2011). Here, aspartic or glutamic acid did not majorly affect Amadori degradation kinetics, but favored carboxymethylation and deglycation (Fig. 7). Basic residues in $i + 4$ position clearly enhanced the degradation of the Amadori moiety (Fig. 7a), but produced lower product amounts that could not be traced back to a

higher product diversity. Whereas spatially proximate histidine has been reported to act as an acid-base-catalyst in the Amadori rearrangement, strongly basic residues such as arginine have been reported to enhance Amadori formation by reducing the lysine's pK_a (Venkatraman et al. 2001). Principally, a catalyst enhancing Amadori rearrangement should exert the same effect on the reverse reaction, which explains the faster deglycation when histidine is positioned *i* + 4. Whereas His could initiate the reverse Amadori rearrangement by both abstracting a proton from C1 or protonating the C2 carbonyl group, Lys and Arg can only interfere in the latter way. Being protonated to high degree at neutral pH, Lys and Arg should be more effective as proton donors compared to His and thus result in even faster Amadori degradation (Fig. 7a).

Conclusion

Amadori modifications are potent CML precursors transforming within minutes efficiently to this AGE during cooking, although it should be noted that most of the Amadori peptide is deglycated to the native sequence. Our results suggest that this transformation being rather due to 'glycooxidation' than 'oxidative glycosylation'. The formation of deglycated peptides and peptides with sugar-related modifications occurred faster than the oxidative damages. Additionally, sugar-related modifications and oxidative damage showed different ROS-dependent kinetics, which might help to group unknown modifications according to their mechanistic origin.

Previous studies, which were conducted at the amino acid level, were extended by the presented glycation system now allowing to study independent reactions at different sites. Compared to a protein, where glycation and glycooxidation are distributed to several residues and thus result in lower modification levels at specific sites, reactions on the peptide level allow to concentrate sugar-related reactions to one residue, which resulted here in the discovery of three modifications (*N*^ε-ethanallyl, *N*^ε-formate, and *N*^ε-methyl lysine) not described in the glycation context before. Furthermore, sequence-dependent degradation of the *N*^ε-fructosyl lysine and product formation was shown here for the first time.

Acknowledgments We thank Mr. Viktor Sekovski and Mr. Marko Damjanovic for their assistance in synthesizing peptides and analyzing some data sets, respectively. Financial support from the Deutsche Forschungsgemeinschaft (HO2222/7-1, FR-3117/2-1) and the European Fund for Regional Structure Development (EFRE, European Union and Free State Saxony; 100055720, 100092961, 100146238) as well as a PhD fellowship from the Ernst Schering Foundation (UG) are gratefully acknowledged. PhD fellowship from the Ernst Schering Foundation (UG), Deutsche Forschungsgemeinschaft (HO2222/7-1, FR-3117/2-1), and European Fund for Regional Structure

Development (EFRE, European Union and Free State Saxony; 100055720, 100092961, 100146238).

Conflict of interest The authors declare no conflict of interest.

Ethical standard The article does not contain any studies with human participants or animals performed by any of the authors.

References

- Ahmed MU, Thorpe SR, Baynes JW (1986) Identification of *N*-epsilon-carboxymethyllysine as a degradation product of fructoselysine in glycated protein. *J Biol Chem* 261:4889–4894
- Ahmed MU, Frye EB, Degenhardt TP et al (1997) *N*-epsilon-(carboxyethyl)lysine, a product of the chemical modification of proteins by methylglyoxal, increases with age in human lens proteins. *Biochem J* 324:565
- Ahmed N, Thornalley PJ, Dawczynski J et al (2003) Methylglyoxal-derived hydroimidazolone advanced glycation end-products of human lens proteins. *Invest Ophthalmol Vis Sci* 44:5287–5292
- Ahmed N, Mirshekar-Syahkal B, Kennish L et al (2005) Assay of advanced glycation endproducts in selected beverages and food by liquid chromatography with tandem mass spectrometric detection. *Mol Nutr Food Res* 49:691
- Akagawa M, Sasaki D, Kurota Y, Suyama K (2005) Formation of alpha-amino adipic and gamma-glutamic semialdehydes in proteins by the Maillard reaction. *Mol React Chem Interface Nutr Aging, Dis* 1043:Asahi Kasei Pharma; Aventis; BASF; Biostratum; Univ
- Akira K, Hashimoto T (2005) Use of C-13 labeling and NMR spectroscopy for the investigation of degradation pathways of Amadori compounds. *Biol Pharm Bull* 28:344
- Biemel KM, Buhler HP, Reihl O, Lederer MO (2001) Identification and quantitative evaluation of the lysine–arginine crosslinks GODIC, MODIC, DODIC, and glucosepan in foods. *Nahrung-Food* 45:210
- Biemel KM, Conrad J, Lederer MO (2002) Unexpected carbonyl mobility in aminoketoses: the key to major Maillard crosslinks. *Angew Chem-Int Ed* 41:801
- Bollineni RC, Fedorova M, Hoffmann R (2011) Identification of carbonylated peptides by tandem mass spectrometry using a precursor ion-like scan in negative ion mode. *J Proteomics* 74:2351–2359
- Brock JWC, Hinton DJS, Cotham WE et al (2003) Proteomic analysis of the site specificity of glycation and carboxymethylation of ribonuclease. *J Proteome Res* 2:506
- Buettner GR, Jurkiewicz BA (1996) Catalytic metals, ascorbate and free radicals: combinations to avoid. *Radiat Res* 145:532
- Cai J, Hurst HE (1999) Identification and quantitation of *N*-(carboxymethyl)valine adduct in hemoglobin by gas chromatography mass spectrometry. *J Mass Spectrom* 34:537
- Cohen MP, Ziyadeh FN, Chen S (2006) Amadori-modified glycated serum proteins and accelerated atherosclerosis in diabetes: pathogenic and therapeutic implications. *J Lab Clin Med* 147:211–219
- Dangles O, Guibe F, Balavoine G et al (1987) Selective cleavage of the allyl and allyloxycarbonyl groups through palladium-catalyzed hydrostannolysis with tributyltin hydride—application to the selective protection–deprotection of amino-acid derivatives and in peptide-synthesis. *J Org Chem* 52:4984–4993
- Davidek T, Clety N, Aubin S, Blank I (2002) Degradation of the Amadori compound *N*-(1-deoxy-D-fructos-1-yl)glycine in aqueous model systems. *J Agric Food Chem* 50:5472–5479
- Dorfman LM, Adams GE (1973) Reactivity of the hydroxyl radical in aqueous solutions

- Frolov A, Hoffmann R (2008) Separation of Amadori peptides from their unmodified analogs by ion-pairing RP-HPLC with heptafluorobutyric acid as ion-pair reagent. *Anal Bioanal Chem* 392:1209
- Frolov A, Singer D, Hoffmann R (2006) Site-specific synthesis of Amadori-modified peptides on solid phase. *J Pept Sci* 12:389
- Frolov A, Schmidt R, Spiller S et al (2014) Arginine-derived advanced glycation end products generated in peptide–glucose mixtures during boiling. *J Agric Food Chem* 62:3626–3635
- Glomb MA, Monnier VM (1995) Mechanism of protein modification by glyoxal and glycolaldehyde, reactive intermediates of the Maillard reaction. *J Biol Chem* 270:10017
- Goldberg T, Cai WJ, Peppas M et al (2004) Advanced glycoxidation end products in commonly consumed foods. *J Am Diet Assoc* 104:1287
- Grillo MA, Colombatto S (2008) Advanced glycation end-products (AGEs): involvement in aging and in neurodegenerative diseases. *Amino Acids* 35:29–36
- Han KK, Richard C, Biserte G (1983) Current developments in chemical cleavage of proteins. *Int J Biochem* 15:875–884
- Hasenkopf K, Ronner B, Hiller H, Pischetsrieder M (2002) Analysis of glycated and ascorbylated proteins by gas chromatography-mass spectrometry. *J Agric Food Chem* 50:5697–5703
- Hayashi T, Namiki M (1980) Formation of 2-carbon sugar fragment at an early stage of the browning reaction of sugar with amine. *Agric Biol Chem* 44:2575
- Heyns K, Noack H (1962) Die Umsetzung Von D-fructose Mit L-lysin Und L-arginin Und Deren Beziehung Zu Nichtenzymatischen Braunungsreaktionen. *Chem Berichte-recueil* 95:720
- Hodge JE (1955) The Amadori rearrangement. *Adv Carbohydr Chem* 10:169
- Jakas A, Horvat S (2003) Study of degradation pathways of Amadori compounds obtained by glycation of opioid pentapeptide and related smaller fragments: stability, reactions, and spectroscopic properties. *Biopolymers* 69:421
- Kahne D, Still WC (1988) Hydrolysis of a peptide-bond in neutral water. *J Am Chem Soc* 110:7529–7534
- Kloepfer A, Spanneberg R, Glomb MA (2011) Formation of arginine modifications in a model system of *N*-alpha-tert-Butoxycarbonyl (Boc)-arginine with methylglyoxal. *J Agric Food Chem* 59:394–401
- Martins SIFS, Van Boekel MAJS (2003) Kinetic modelling of Amadori *N*-(1-deoxy-D-fructos-1-yl)-glycine degradation pathways. Part II—kinetic analysis. *Carbohydr Res* 338:1665
- Martins SIFS, Marcelis ATM, van Boekel MAJS (2003) Kinetic modelling of Amadori *N*-(1-deoxy-D-fructos-1-yl)-glycine degradation pathways. Part I—reaction mechanism. *Carbohydr Res* 338:1651
- Meltretter J, Pischetsrieder M (2008) Application of mass spectrometry for the detection of glycation and oxidation products in milk proteins. *Mail React Recent Adv Food Biomed Sci Ann New York Acad Sci* 1126:134
- Meltretter J, Birlouez-Aragon I, Becker CM, Pischetsrieder M (2009) Assessment of heat treatment of dairy products by MALDI-TOF-MS. *Mol Nutr Food Res* 53:1487
- Milic I, Hoffmann R, Fedorova M (2013) Simultaneous detection of low and high molecular weight carbonylated compounds derived from lipid peroxidation by electrospray ionization-tandem mass spectrometry. *Anal Chem* 85:156–162
- Miyata T, Sprague SM (1996) Advanced glycation of beta(2)-microglobulin in the pathogenesis of bone lesions in dialysis-associated amyloidosis. *Nephrol Dial Transplant* 11:86–90
- Rabbani N, Thornalley PJ (2012) Methylglyoxal, glyoxalase 1 and the dicarbonyl proteome. *Amino Acids* 42:1133–1142
- Schiekofer S, Andrassy M, Chen J et al (2003) Acute hyperglycemia causes intracellular formation of CML and activation of ras, p42/44 MAPK, and nuclear factor kappa B in PBMCs. *Diabetes* 52:621
- Schwietzke U, Malinowski J, Zerge K, Henle T (2011) Quantification of Amadori products in cheese. *Eur Food Res Technol* 233:243
- Simon JA, Hudes ES (1999) Relation of serum ascorbic acid to serum vitamin B-12, serum ferritin, and kidney stones in US adults. *Arch Intern Med* 159:619–624
- Smuda M, Voigt M, Glomb MA (2010) Degradation of 1-Deoxy-D-erythro-hexo-2,3-diulose in the presence of lysine leads to formation of carboxylic acid amides. *J Agric Food Chem* 58:6458
- Stadtman ER (1993) Oxidation of free amino-acids and amino-acid-residues in proteins by radiolysis and by metal-catalyzed reactions. *Annu Rev Biochem* 62:797–821
- Staempfli AA, Blank I, Fumeaux R, Fay LB (1994) Study on the decomposition of the Amadori compound *N*-(1-deoxy-D-fructos-1-yl)-glycine in model systems—quantification by fast-atom-bombardment tandem mass-spectrometry. *Biol Mass Spectrom* 23:642–646
- Statland BE, Winkel P, Bokelund H (1976) variation of serum iron concentration in young healthy men—within-day and day-to-day changes. *Clin Biochem* 9:26
- Venkatraman J, Aggarwal K, Balaram P (2001) Helical peptide models for protein glycation: proximity effects in catalysis of the Amadori rearrangement. *Chem Biol* 8:611
- Watkins NG, Thorpe SR, Baynes JW (1985) Glycation of amino-groups in protein—studies on the specificity of modification of nase by glucose. *J Biol Chem* 260:10629–10636
- Wells-Knecht MC, Thorpe SR, Baynes JW (1995) Pathways of formation of glycoxidation products during glycation of collagen. *Biochemistry* 34:15134
- Wolff SP, Dean RT (1987) Glucose autooxidation and protein modification—the potential role of autooxidative glycosylation in diabetes. *Biochem J* 245:243
- Yeboah FK, Alli I, Yaylayan VA (1999) Reactivities of D-glucose and D-fructose during glycation of bovine serum albumin. *J Agric Food Chem* 47:3164–3172
- Zhang Q, Monroe ME, Schepmoes AA et al (2011) Comprehensive identification of glycated peptides and their glycation motifs in plasma and erythrocytes of control and diabetic subjects. *J Proteome Res* 10:3076
- Zhang PJ, Zhao ZG, Yu SJ, He SZ (2012) Degradation of *N*-(1-Deoxy-D-xylulos-1-yl)glycine and *N*-(1-Deoxy-D-xylulos-1-yl)proline using thermal treatment. *Int J Food Sci Technol* 47:475
- Zyzak DV, Richardson JM, Thorpe SR, Baynes JW (1995) Formation of reactive intermediates from Amadori compounds under physiological conditions. *Arch Biochem Biophys* 316:547